

## Extended-Bandwidth Microstrip Circular Patch Antenna for Dual Band Applications

A. H. Majeed<sup>1</sup>, K. H. Sayidmarie<sup>2</sup>

<sup>1</sup>College of Engineering, Al-Nahrain University, Baghdad, Iraq

<sup>2</sup>College of Electronic Engineering, Ninevah University, Mosul, Iraq

---

### Article Info

#### Article history:

Received Oct 11, 2017

Revised Dec 28, 2017

Accepted Jan 10, 2018

#### Keyword:

Circular patch antenna

Dual-band antenna

Extended bandwidth

Proximity coupling

Stub matching

---

### ABSTRACT

This paper presents a new wideband microstrip circular patch antenna (MCPA) fed by proximity-coupled line with double-stub matching to achieve dual-band operation. Bandwidth extension is achieved by exciting higher-order modes in the circular radiating patch, and using two stubs to achieve adequate matching across the obtained two bands. The characteristics of the antenna such as reflection coefficient, impedance bandwidth, gain and radiation pattern are investigated and optimized through parametric studies using the CST Microwave Studio Suite. The antenna achieved a large relative bandwidth of 45.16% at the upper band, while the lower one has 10.3% relative bandwidth. The maximum achieved gain of the dual-band antenna in the 5.8GHz band is 4.62dBi while it is 4.85dBi in the upper band. The antenna has an overall size of  $30 \times 30 \times 3.2 \text{mm}^3$  corresponding to  $0.58\lambda \times 0.58\lambda \times 0.062\lambda$  at the lower band of 5.8 GHz. The proposed antenna should be useful for WLAN and X-band communication systems.

Copyright © 2018 Institute of Advanced Engineering and Science.

All rights reserved.

---

### Corresponding Author:

K. H. Sayidmarie,

College of Electronic Engineering,

Ninevah University,

Mosul, Iraq.

Email: kh.sayidmarie@uoninevah.edu.iq

---

## 1. INTRODUCTION

Microstrip patch antennas (MPAs) have various advantages such as low profile, light weight and being conformal to hosting surfaces. Thus, they are used in wide range of applications like mobile communication systems, global positioning systems (GPS), microwave sensors, wireless local area networks (WLAN), etc [1]. However, microstrip antennas suffer from the small working bandwidth of less than about 10%. Therefore, various techniques have been proposed for bandwidth extension of the microstrip antennas. The proximity coupling was found to achieve a 13% relative bandwidth in rectangular patch antenna [2]. This technique has other benefits such as ease of matching and fabrication compared to the other feeding schemes. Another proposed solution was the use of a parasitic resonator coupled to the patch forming a wideband stacked microstrip patch antenna [3]. In [4] a special shape antenna consisting of a rectangular patch tapered at two corners and loaded with three notches and one slot was presented. A proper selection of dimensions and positions of the slot and notch have led to 30.5% relative bandwidth.

The realization of a dual-band operation can be considered as another scheme to achieve wider bandwidth. A popular method for designing a single-fed dual-band antenna is to stack two resonating structures of proper dimensions to excite two fundamental modes corresponding to the desired bands [5], [6]. The height between the resonators needs optimization to ensure impedance matching and adequate bandwidth of the antenna. The achieved bandwidths in [5] were 8.3% and 7% for the lower and upper bands respectively. Slightly larger bandwidths of 10.64% and 8.82% for the  $L_1$  and  $L_2$  GPS bands respectively were obtained in [6]. However, these acquired benefits are on the account of size increase. In another design with

inserting a slot on the ground plane and a stacked patch supported by a wall, the bandwidth was increased up to 25% [7]. A stacked patch antenna based on aperture coupling and asymmetry feeding technique was presented in [8]. A cross-shape aperture imbedded in the ground plane with asymmetry feeding structure provided a relative wideband electromagnetic coupling. The experimental results showed that an impedance bandwidth of 35.3% was achieved [8]. In [9] a dual-band GPS antenna incorporating a proximity-coupled feed was proposed. The radiating element is a circular patch with a cross-slot and a ring-slot to excite the  $TM_{11}$  mode at the GPS  $L_1$  and  $L_2$  bands, and the measured bandwidths were 6.1% and 3.7% respectively. A novel feeding system for microstrip radiators which is based on an electromagnetic coupling was presented in [10]. The single feed line is ended by two arms which hug the patch near the edge in a symmetrical manner with a capacitive gap to the two adjacent sides of the rectangular patch in order to initiate circular polarization. The result of the developed prototype was a 3dB axial ratio bandwidth of 3.9%. The achieved impedance bandwidth was 4.9%. A broadband proximity-coupled dual-polarized microstrip antenna with an L-shape backed cavity was presented [11]. The L-shape cavity enhances the feed coupling and thus broadens the bandwidth. A prototype antenna with optimized parameters showed relative bandwidth of more than 30% (8.2–11.4 GHz) and the two port isolation is larger than 20 dB. The antenna has three substrates and a thick ground plane leading to dimensions of 28X28X9.4 mm<sup>3</sup>. Slots and rings in the circular microstrip patch were also used to achieve multiband operation [12], [13].

A compact wideband dual-frequency microstrip antenna is proposed in [14]. The antenna has an offset microstrip-fed line and a strip close to the radiating edges in the circular slot patch, and achieved bandwidths of 26.2% and 22.2% for the two bands. A stacked dual-layer circular patch antenna with enhanced bandwidth is recently proposed in [15]. The antenna has a slotted circular patch, a parasitic circular patch on the top layer and showed a 25% relative bandwidth. In [16] using probe-fed stacked circular patches and optimization of the dielectric constants of the two substrates it was found that bandwidths up to 30% can be achieved. The lower patch is probe-fed with high dielectric constant substrate while the upper one is capacitively coupled through. However, bandwidth expansion is achieved on the account of increased thickness. The antenna in [16] has thickness of 31% of the circular patch diameter leading to a large antenna volume.

This paper presents a new wideband microstrip circular patch antenna (MCPA) fed by proximity-coupled line with double-stub matching to achieve dual-band operation. The proposed antenna is analyzed and optimized using the CST Microwave Studio Suite. The proposed antenna is then developed to exhibit dual-band of WLAN and X-Band operation. The higher band is achieved by exciting higher modes in the circular radiating patch. To furnish proper matching for the higher band, two stubs are connected to both sides of the feeding line. The two-stub technique can offer matching across a wide band that covers more than one resonating mode of the circular patch antenna. Section 2 discusses the theoretical aspects of the circular patch antenna. Section 3 demonstrates the parametric study of the antenna performance, and the optimized Antenna-I is presented in Section 4. The development of Antenna-I to a dual-band antenna II is discussed in Section 5. Finally, the conclusions are given in Section 6.

## 2. ANTENNA GEOMETRY

Figure 1 shows the configuration of the proximity-coupled microstrip circular patch antenna (Antenna-I) with detailed dimensions and parameters. The antenna consists of a grounded substrate of dimensions (30 × 30) mm<sup>2</sup> where a microstrip feed line is printed. The microstrip line is  $W_f = 3.1$ mm wide and  $L_f = 16$ mm long and is located at a distance of  $x_1 = -2.4$ mm from the center of the circular patch. The substrate of this layer is FR4 (glass epoxy) with dielectric constant of  $\epsilon_r = 4.3$  and thickness of  $h = 1.6$  mm. Above this layer, there is another dielectric laminate of the same material and thickness as the first layer with a microstrip patch etched on its top surface. The end of the feed line is shifted from the center of the circular patch by a distance of  $y = 1.5$ mm. A copper film of thickness 0.05mm was used as the ground plane of the antenna. The electromagnetic coupling between the feed line and the patch results in power transfer, as opposed to a direct contact [17].

The patch used in this paper is of a circular shape whose resonance frequency  $f_{nm}$  can be calculated using the cavity model as [18], [19]:

$$f_{nm} = \frac{\chi_{nm} c}{2\pi a_e \sqrt{\epsilon_r}} \quad (1)$$

where  $\chi_{nm}$  is the  $m^{\text{th}}$  root of the Bessel function derivative  $J'_n(ka)$ ,  $\epsilon_r$  is the relative permittivity of the substrate, and  $c$  is the speed of light. The effective radius  $a_e$  of the radiating circular patch is to compensate

for the fringing field effect along the edge of the circular disk. For the  $TM_{11}$  mode, it was suggested that  $a_e$  can be given by [18, 19]:

$$a_e = a \sqrt{\left\{ 1 + \frac{2h}{\pi a \epsilon_r} \times \left[ \ln(\pi a / 2h) + 1.7726 \right] \right\}} \quad (2)$$

where  $h$  is the height of substrate and  $a$  is the actual radius of the circular patch. Thus using Equation (1) and Equation (2), it was found that a resonant frequency of 5.8 GHz is obtained for a 6mm patch radius.

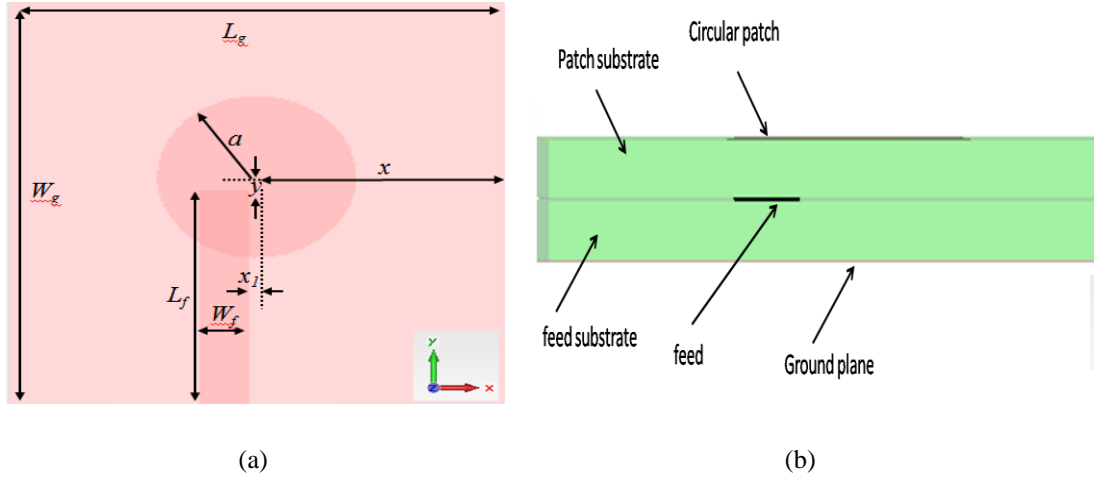


Figure 1. Geometry of Antenna I; (a) Top view , (b) Side view

### 3. PARAMETRIC STUDY AND OPTIMIZATION

In this section, the antenna structure is analyzed and optimized using the CST Microwave Studio Suite 2011, which is an electromagnetic simulator based on the finite integration technique [20]. The analysis of the antenna for different parameter values has been carried out by varying one parameter while the other ones are kept constant. The optimized dimensions of Antenna-I are shown in Table 1. Figure 2 shows the simulated reflection coefficient of the optimized Antenna-I as a function of frequency. It is clear from this figure that the antenna has a relative impedance bandwidth of 9.5% or 0.55GHz for reflection coefficient  $\leq -10$ dB. Figure 3 shows the simulated realized gain of the optimized antenna as a function of frequency. The antenna has a maximum gain of 4.62dB<sub>i</sub> across the band of interest.

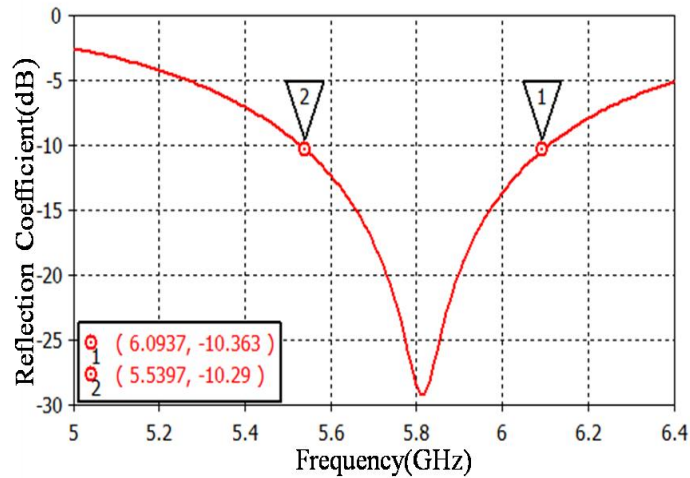


Figure 2. Simulated reflection coefficient of optimized Antenna-I as a function of frequency

Table 1. Optimized parameters of the Antenna-I. All dimensions are in millimeters.

$W_g$	$L_g$	$L_f$	$W_f$	$a$	$x$	$x_l$	$y$
30	30	16	3.1	6	15	-2.4	1

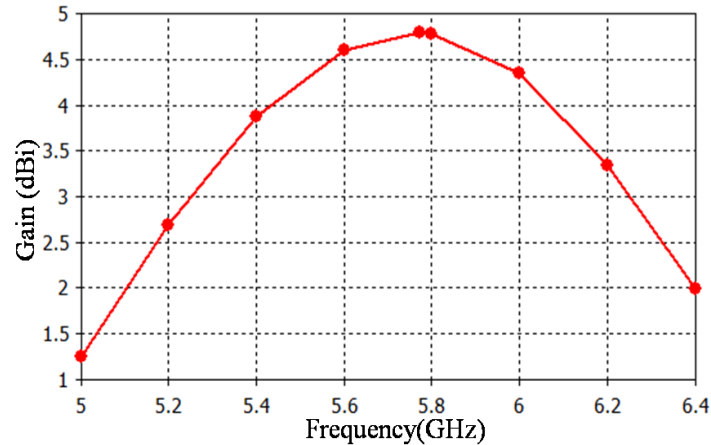


Figure 3. Simulated realized gain of optimized Antenna-I as a function of frequency

#### 4. BANDWIDTH EXTENSION

The proposed Antenna-I analyzed in the former sections was developed to obtain a dual-band operation with extended bandwidth. For this purpose, the higher resonance modes of the circular patch have been utilized. However, to excite these modes properly matching of the proximity coupled circular disk needs to be improved. Therefore, a double-stub matching network was added to the feed line of Antenna-I to form a proposed Antenna-II whose geometry is shown in Figure 4.

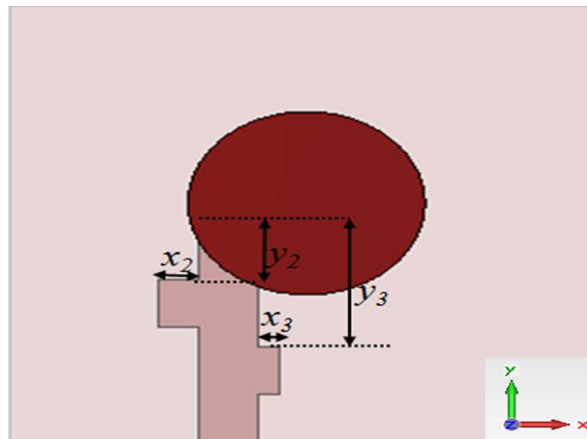


Figure 4. Geometry of the proposed dual-band (Antenna-II) with the added double-stub for matching

Figure 5 shows the variation of the simulated reflection coefficient of Antenna-II with frequency for various separations of the upper stub from the end of the feed line ( $y_2$ ). The results show two bands; the former band (before adding the stubs) is at around 5.8GHz and a new (upper band) across the frequency from 8.5 to 13 GHz. The figure also shows that the matching is improved with increasing the separation of the upper stub from the end of the feed line and the width of each band is increased. A separation of  $y_2 = 4\text{mm}$  was found to give the best results. During this simulation, the length of the lower stub was fixed at  $x_3 = 1\text{mm}$  at a distance of  $y_3 = 8.4\text{mm}$  from the upper end of the feed line and the length of the upper stub at  $x_2 = 2\text{mm}$ .

Figure 6 shows the simulated reflection coefficient of Antenna-II as a function of frequency for various lengths of the upper stub ( $x_2$ ). It is clear from this figure that the matching is improved and the bandwidth is increased for the upper band with increasing the length of upper stub from 1mm to 2mm. After 2mm i.e. at  $x_2 = 2.5$ mm, the situation gets worse in terms of matching and bandwidth. For the lower band, the figure shows that the resonance frequency shifts towards left and the matching degrades slightly with increasing in  $x_2$ . Thus, a length of  $x_2 = 2$ mm for the upper stub was found to give the best result. During this simulation, the length of the lower stub was kept equal to  $x_3 = 1$ mm at a distance of  $y_3 = 8.4$ mm from the lower end of the feed line and the distance of the upper stub is  $y_2 = 4$ mm from the upper end of the feed line.

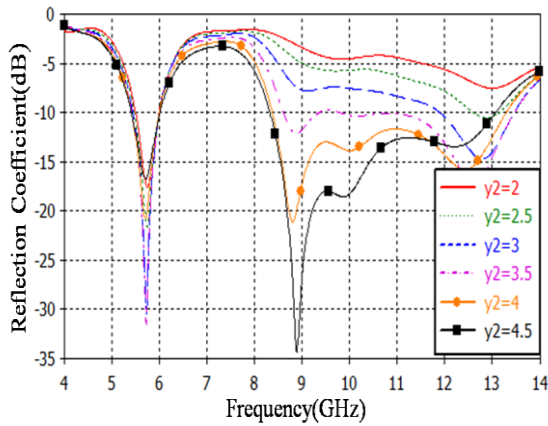


Figure 5. Simulated reflection coefficient of Antenna-II as a function of frequency for various separations of the upper stub from the end of the feed line ( $y_2$ ).  $x_3=1.25$ mm, and  $y_3=7.4$ mm

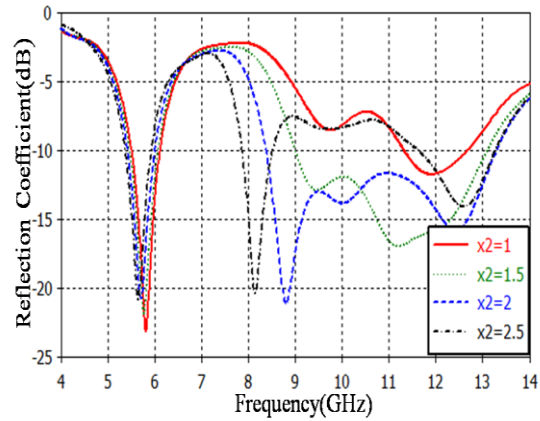


Figure 6. Simulated reflection coefficient of Antenna-II as a function of frequency for various lengths of the upper stub ( $x_2$ ).  $x_3 = 1.25$ mm, and  $y_3 = 7.4$ mm

Figure 7 shows the simulated reflection coefficient of Antenna-II as a function of frequency for various separations of the lower stub from the end of the feed line ( $y_3$ ). It is clear from the figure that there is shifting in the upper band towards left with increasing in the separation of the lower stub from the feed line's upper edge with decreasing in bandwidth. The matching is also improved for the lower band with increasing  $y_3$  with a little effect on the bandwidth. It was found that the best separation of the lower stub from the end of the feed line is  $y_3 = 8.4$ mm. The length of the upper stub was kept equal to  $x_2 = 2$ mm at a distance of  $y_2 = 4$ mm from the upper end of the feed line, and the length of the lower stub is  $x_3 = 1.25$ mm.

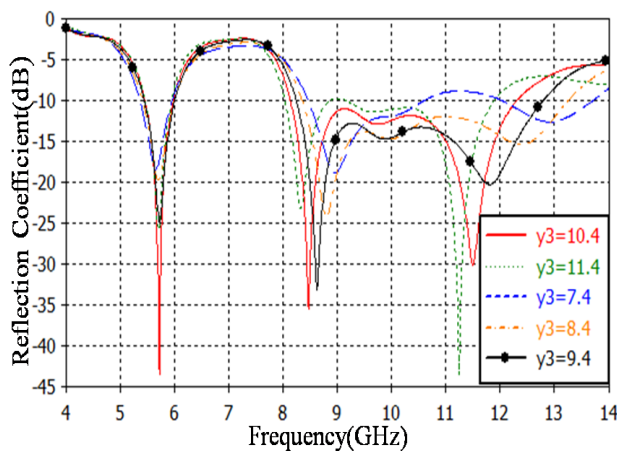


Figure 7. Simulated reflection coefficient of Antenna-II as a function of frequency for various separations of the lower stub from the end of the feed line ( $y_3$ ).  $x_2 = 2$ mm, and  $y_2 = 4$ mm

Figure 8 shows the simulated reflection coefficient of Antenna-II as a function of frequency for various lengths of the lower stub ( $x_3$ ). The figure shows that for the upper band the matching gets worse and the bandwidth decreases with increasing the length of the lower stub, while there is a little effect on the lower band. The best results were obtained for lower stub length of  $x_3 = 1$ mm. The length of the upper stub was kept equal to  $x_2 = 2$ mm at a distance of  $y_2 = 4$ mm from the upper end of the feed line and the distance of the lower stub is  $y_3 = 8.4$ mm from the upper end of the feed line.

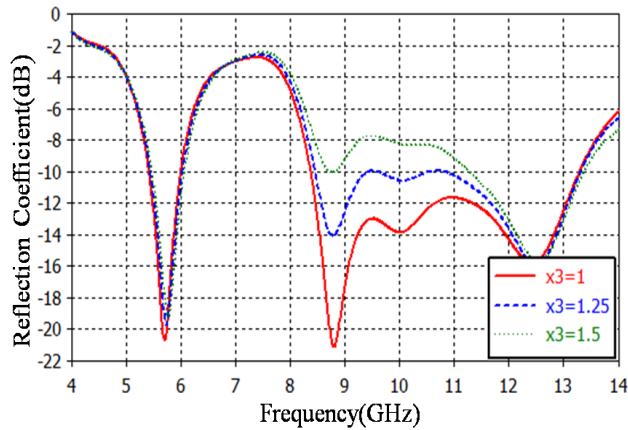


Figure 8. Simulated reflection coefficient of Antenna- II as a function of frequency for various lengths of the lower stub ( $x_3$ ).  $x_2 = 2$ mm, and  $y_2 = 4$ mm

The optimum parameters for Antenna-II are listed in Table 2. Figure 9 shows a comparison between the simulated reflection coefficients of the optimized Antenna-I and Antenna-II. This figure shows that adding the impedance matching network to Antenna-I (to obtain Antenna-II) has improved its characteristics in terms of getting an upper band with a wider bandwidth. Antenna-II has a relative bandwidth of 10.3% for the lower band which is larger than that for Antenna-I. The upper band of Antenna-II covers the whole X-Band corresponding to a much larger relative bandwidth of (45.16%).

Table 2. Optimized parameters of the Antenna-II, all dimensions are in millimeters

$W_g$	$L_g$	$L_f$	$W_f$	$a$	$x$	$x_1$	$y$	$x_2$	$x_3$	$y_2$	$y_3$
30	30	16	3.1	6	15	-2.4	1	2	1	4	8.4

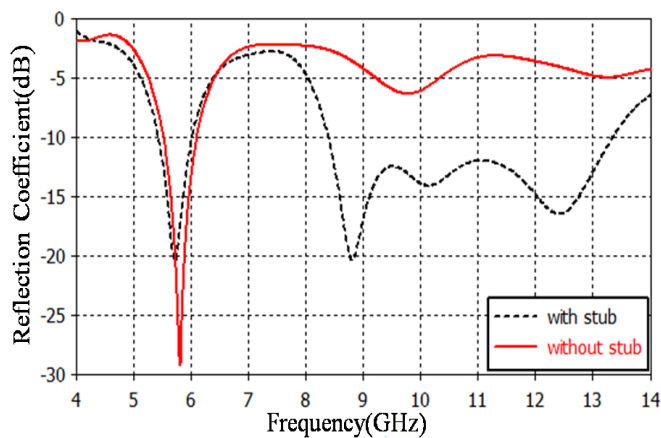


Figure 9. Comparison between the simulated reflection coefficient of Antenna-I and Antenna-II as a function of frequency

The achievement of the second band can be explained through the following. The resonance frequencies  $f_{nm}$  of the circular patch ( $a = 6\text{mm}$ ) for the first 3 modes were calculated using Equation (1) and Equation (2), and the obtained results are shown in Table 3. Figure 9 clearly shows that before the addition of the two stubs (Antenna-I) the lowest resonance mode  $TM_{11}$  has a frequency of 5.80 GHz. The other two higher modes ( $TM_{21}$  and  $TM_{02}$ ) should appear at frequency of 9.518 GHz and 11.941 GHz according to Equation (1) and Equation (2). The simulated results of Figure 9 show that, for Antenna-I, these two modes have appeared at 9.77GHz and 13.21 GHz. They look partially matched as seen from the shallow dips (around -5dB) in the reflection coefficient response. However, after adding the two stubs (Antenna-II), the upper two modes have appeared at 8.80GHz and 12.37GHz. The two modes have merged together to form a joined band covering a wide range extending from 8.4 GHz to 13.4 GHz.

It should be noted that these calculations are based on the assumption that the resonating circular patch is not accompanied with the feed line (the cavity model). However, the addition of the feed line for coupling will affect the values of the resonating frequency. In this design, the microstrip feed line is partially inserted between the circular patch and the ground plane. Table 3 shows that the simulated frequencies for Antenna-I are within less than 7% of those estimated by Equation (1) and Equation (2). These results show that Equation (1) and Equation (2) can give good estimates of the resonance frequencies. In the design process, better tuning of the frequencies to the desired values can be obtained through the analysis of the CST Microwave Studio suite [18].

Table 3. Calculated values of the resonance frequencies of the lowest three modes of the circular patch antenna ( $a = 6\text{mm}$ ,  $h = 3.2\text{mm}$ )

frequency $f_{nm}$ GHz	Mode	$TM_{11}$	$TM_{21}$	$TM_{02}$
	$\chi_{nm}$	1.841	3.0542	3.8317
from Eq. (1) & Eq. (2)		5.738	9.518	11.941
simulated Antenna-I		5.80	9.77	13.21
simulated Antenna-II		5.73	8.80	12.37

Figure 10 shows a comparison between the realized gains of the optimized Antenna-I and Antenna-II. The addition of the two stubs has slightly increased the gain at the lower band, while has led to an upper band of a minimum gain of 2 dB<sub>i</sub> across the X-Band. It is clear from this figure that Antenna-I has a maximum gain of 4.62dB<sub>i</sub> at 5.79GHz while Antenna-II has a maximum gain of 4.88dB<sub>i</sub> at 5.72GHz lower band and a maximum gain of 3.74dB<sub>i</sub> at 11GHz for the upper wider band.

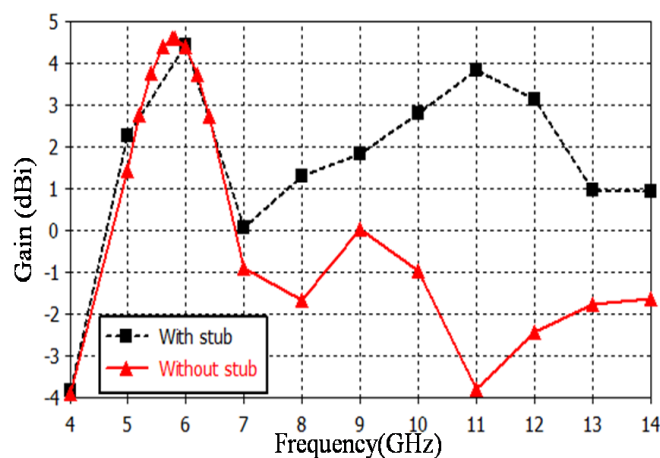


Figure 10. Comparison between the realized gain of Antenna-I and Antenna-II as a function of frequency

In order to validate the results obtained by CST MWS the performance of the optimized antenna II was simulated using EM simulator based on HFSS. Figure 11 compares the obtained reflection coefficient of the optimized antenna II from the two simulation suits. Table 4 depicts a quantitative comparison of the two frequency responses. From Figure 11 and Table 3, a good agreement between two simulation results is observed. A slight difference between the two results can be attributed to different numerical techniques employed by the two simulators.

Table 4. Comparison of CST and HFSS simulated results of the optimized antenna II

Simulator	Lower band			Upper band		
	$f_l$ (GHz)	$f_h$ (GHz)	BW %	$f_l$ (GHz)	$f_h$ (GHz)	BW %
CST	5.448	6.038	10.27	8.400	13.289	45.10
HFSS	5.604	6.194	10.02	8.427	13.744	47.96

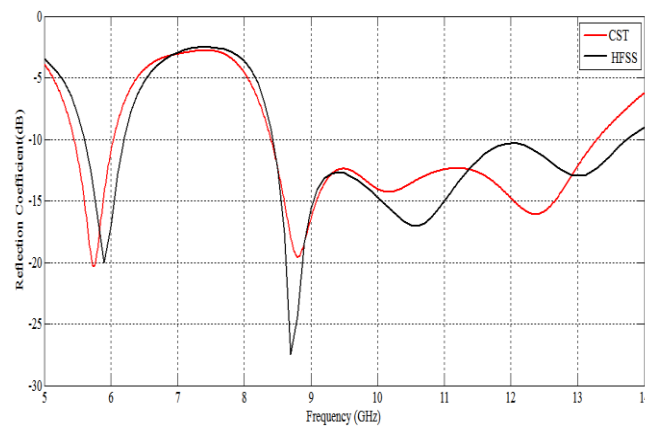


Figure 11. CST MWS and HFSS simulated reflection coefficient of the optimized antenna II

The simulated realized gain against frequency obtained from the CST and HFSS software packages are shown in Figure 12 and Table 5 summarizes the result obtained from this figure.

Figure 13 shows the 3-D radiation patterns of Antenna-II for four selected frequencies (5.72GHz, 8.81GHz, 10.14GHz and 12.4GHz) which satisfy the lowest reflection coefficient across the two satisfied bands. The far field has a maximum along the normal direction to the radiating disk with good coverage across the half plane. The antenna shows a good front to back ratio of better than 20 dB.

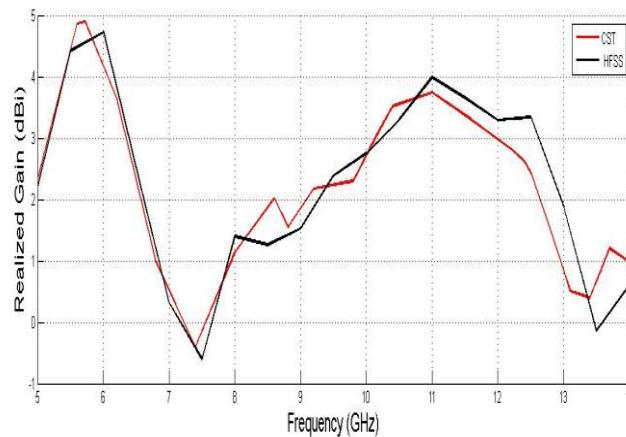


Figure 12. CST MWS and HFSS simulated realized gain of the optimized antenna II

Table 5. Comparison of CST and HFSS simulated realized gain of Optimized antenna II

Simulator	Lower band		Upper band	
	Min. gain (dB <sub>i</sub> )	Max. gain (dB <sub>i</sub> )	Min. gain (dB <sub>i</sub> )	Max. gain (dB <sub>i</sub> )
CST	3.974	4.859	2.015	3.742
HFSS	4.456	4.744	1.996	4.00

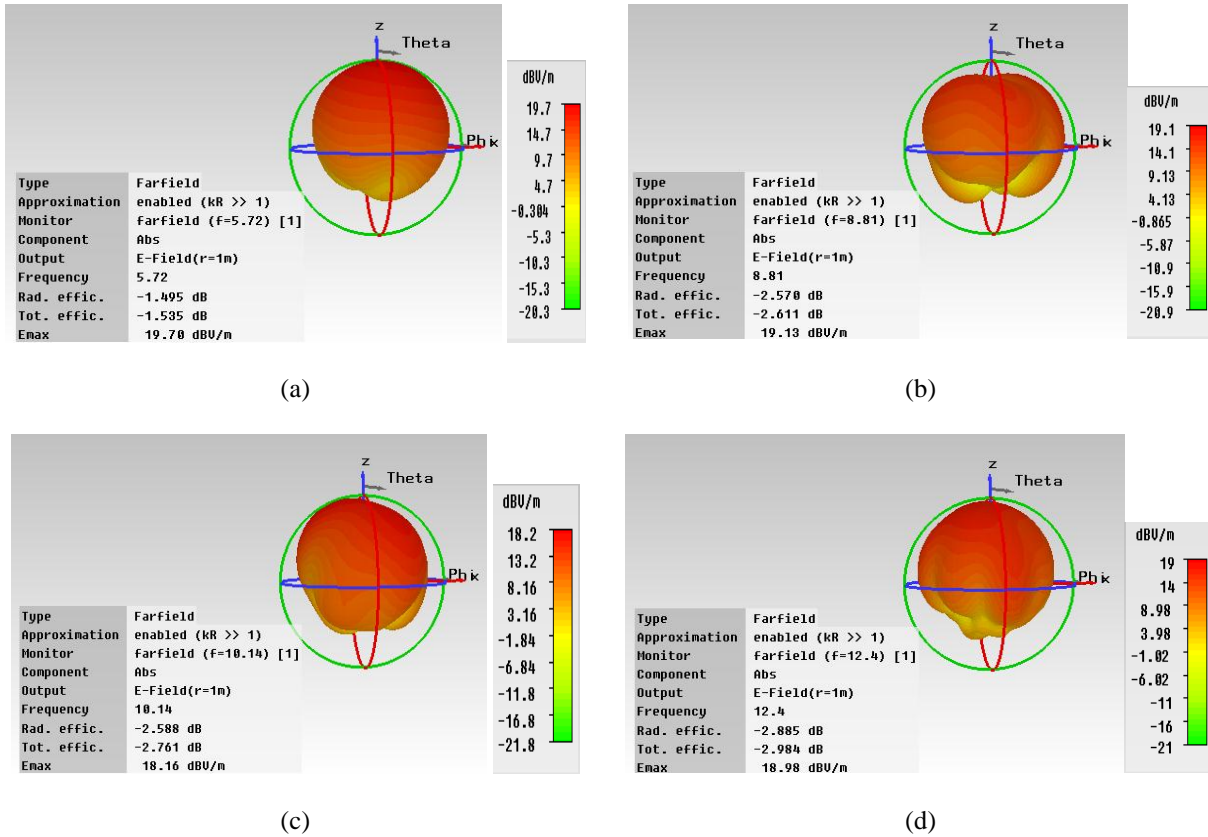


Figure 13. Simulated 3-D radiation patterns of Antenna-II for (a) 5.72GHz, (b) 8.81GHz, (c) 10.14GHz and (d) 12.4GHz

5. COMPARISON WITH OTHER WORKS

The obtained results of the proposed Antenna-I and Antenna-II are compared with those of the antennas presented in [1-11], [14-16], [21]. The comparison takes into consideration the total substrate dimensions and the volume of the antenna, frequency range, bandwidth, gain, as shown in Table 4. The dielectric constant of the substrate is also listed to show fair comparison. At a given operating frequency, lower dielectric constant of the substrate leads to larger bandwidth and larger size. From Table 4, it can be noticed that the dimensions and volume of the proposed Antenna-I and Antenna-II are much smaller than those presented in [1-14], but slightly larger than that in [21]. The listed dimensions in [21] are those of the printed patch and the dimensions of the ground plane are not given in [21] but they are obviously larger. The bandwidth of the proposed antenna2 is much better than most of the listed antennas. The gain of Antenna-I and Antenna-II are competitive with those of the other antennas as regards to its small size.

## 6. CONCLUSION

In this paper, a proximity-fed microstrip circular patch antenna is proposed to achieve dual-band operation with a wider bandwidth. The antenna has been designed to operate in more than one resonating mode and the bandwidth enhancement is achieved by using a two-stub matching network on the microstrip feed line. Simulation results showed that the proposed antenna covers two bands of frequency. The frequency range of the first band is from 5.43 GHz to 6.02 GHz (10.3% relative bandwidth) with a minimum reflection coefficient of -20.45dB at 5.72GHz. The second band covers a wide frequency range from 8.4GHz to 13.3GHz (45.16% relative bandwidth). The double-stub matching has facilitated the utilization of two higher-modes for bandwidth extension of the circular microstrip antenna that is known by its narrow bandwidth. The maximum achievable gain of Antenna-II in the first band is 4.62dB; while it is 4.85dB; in the second band. The antenna offers low profile dual-band, high gain and compact size which are favorable features for Wi-Fi and X-band broadband applications.

## REFERENCES

- [1] Singh A, Ansari JA, Aneesh M, Sayeed S. "L-strip proximity fed gap coupled compact semi-circular disk patch antenna". *Alexandria Engineering Journal*, 2014; Vol. 53: 61–67.
- [2] Pozar DM, Kaufman B. "Increasing the bandwidth of a microstrip antenna by proximity coupling". *Electronics Letters*, 1987; Vol. 23 (8): 368-369.
- [3] Anguera J, Puente C, Borja C. "Dual frequency broadband microstrip antenna with a reactive loading and stacked elements". *Progress in Electromagnetics Research Letters*, 2009; Vol. 10: 1-10.
- [4] Kamakshi KM, Singh A, Aneesh M, Ansari JA. "Novel design of microstrip antenna with improved bandwidth". *International Journal of Microwave Science and Technology*, 2014; Vol. 2014, Article ID 659592, 7 pages.
- [5] Zhou Y, Chen C-C, Volakis JL. "Dual-Band proximity-fed stacked patch antenna for Tri-Band GPS applications". *IEEE Transactions on Antennas and Propagation*, 2007; Vol. 55 (1): 220 – 223.
- [6] Wang Y, Feng J, Cui J, Yang X. "A dual-band circularly polarized stacked microstrip antenna with single-fed for GPS applications". *International Symposium on Antenna Propagation and EM Theory*, 2008; ISAP2008: 108–110.
- [7] AbuTarboush HF, Al-Raweshidy HS, Nilavalan R. "Bandwidth enhancement for microstrip patch antenna using stacked patch and slot". *IEEE International Workshop on Antenna Technology, iWAT 2009*, 2-4 March 2009.
- [8] Fang, Q., and Lizhong, S., *Wideband Duallinear Polarized Stacked Patch Antenna with Asymmetry Feeding*, *TELKOMNIKA (Telecommunication Computing Electronics and Control)*, 2014, Vol 12 (1) : 106-112
- [9] Pham N, Chung JY, Lee B. "A Proximity-Fed antenna for dual-band GPS receiver", *Progress In Electromagnetics Research C*, 2016; Vol. 61: 1–8.
- [10] Torres E, Marante F, Tazón A, Vassal'lo J. "New microstrip radiator feeding by electromagnetic coupling for circular polarization". *International Journal of Electronics and Communications (AEÜ)*, 2015; Vol. 69 (12): 1880-1884.
- [11] Liu Y, Chen S, Ren Y, Cheng J, Liu Q. "A broadband proximity-coupled dual-polarized microstrip antenna with L-shape backed cavity for X-band applications". *International Journal of Electronics and Communications (AEÜ)*, 2015; Vol. 69 (9): 1226-1232.
- [12] Wahab A, Xu J. "U-slot Circular Patch Antenna for WLAN Application", *TELKOMNIKA (Telecommunication Computing Electronics and Control)*, 2015, Vol 14 (2): 323-328.
- [13] Rajni R, Kaur G, Marwaha A. "Metamaterial Inspired Patch Antenna for ISM Band by Adding Single-Layer Complementary Split Ring Resonators", *International Journal of Electrical and Computer Engineering (IJECE)* 2015, Vol 5 (6) : 1328-1335
- [14] Tiang JJ, Islam MT, Misran N, Mandeep JS, "Circular microstrip slot antenna for dual-frequency RFID application", *Progress In Electromagnetics Research*, 2011; Vol. 120 : 499-512.
- [15] Chen J, Liu J. "A new broadband dual-layer monopolar circular patch antenna with slot coupling". *Microwave and Optical Technology Letters*, 2017; Vol. 59 (1): 40-43.
- [16] Mitchell A, Lech M, Waterhouse RB. "Search for high-performance probe-fed stacked patches using optimization". *IEEE Transactions on Antennas and Propagation*, 2003; Vol. 51(2): 249-255.
- [17] Sastry IV, Sankar K. "Proximity coupled rectangular microstrip antenna with X-slot for WLAN Application". *Global Journal of Researches in Engineering*, 2014; Vol. 14, Issue 1, Ver. 1.0: 38-42.
- [18] Balanis CA. "Antenna theory, analysis and design". 3<sup>rd</sup> Edition, John Wiley & Sons, 2010: 811-876.
- [19] Garg R, et al., "Microstrip antennas design handbook", Chapter 5, Artech House, 2001.
- [20] "CST: Computer simulation technology based on FDTD method", CST Computer Simulation Technology AG, 2011.
- [21] Abdelaziz, AA. "Bandwidth enhancement of microstrip antenna". 2006; *Progress In Electromagnetics Research*, Pier 63: 311–317.

**BIOGRAPHIES OF AUTHORS**

**Dr Asmaa H. Majeed** received B.Sc. Degree in Electronic and Communication from the Department of Electrical Engineering/University of Technology /Baghdad /Iraq, then M.Sc degree in Electronic and Communication from the Department of Electrical Engineering / Baghdad University/Baghdad /Iraq. Received Ph.D. Degree in Electronic and Communication from the Department of Electrical Engineering/Busrah University /Busrah /Iraq. She is having around 14 years of Teaching Experience. She is member of the teaching staff at the Department of Laser and Optoelectronic Engineering/College of Engineering/ Al-Nahrain University/ Iraq. She has published 13 papers in national and international journals/conferences. Her research interests include the analysis and design of printed antennas.



**Prof Khalil Sayidmarie** received the B.Sc. degree with first class honors in Electronic & Communication Engineering from Mosul University, Iraq, in 1976, and Ph.D. Degree in Antennas & Propagation from Sheffield University/ U.K. in 1981. Then he joined the College of Engineering at Mosul University in 1983, and was promoted to full professor on 1992. He worked as head of electrical engineering department for 9 years. He was a cofounder of the College of Electronic Engineering at Mosul University. He has been Professor of communication engineering at that college. Sayidmarie served as Prof. of communication engineering at the College of Engineering/ University of Amman Al-Ahliyya/ Jordan from Oct 2006 to Sept. 2009. He is prof of communication engineering at the college of electronic engineering/ Ninevah University. He has supervised 38 MSc and PhD theses and published more than 120 papers.